

## Electronic Supporting Information

### Second-order differential accelerators based on the geometry of equilibrium for thermodynamic calculations. Part I. Pure fluids

Héctor Quinteros-Lama<sup>a</sup>, José Matías Garrido<sup>b</sup>, Ilya Polishuk<sup>c</sup>

<sup>a</sup>School of Engineering, Universidad de Talca. Merced 437, 3341717, Curicó, Chile

<sup>b</sup>Department of Chemical Engineering, Universidad de Concepción, Concepción 4070386, Chile

<sup>c</sup>Department of Chemical Engineering, Biotechnology and Materials, Ariel University, 40700, Ariel, Israel

#### S1. Legendre transforms for the displacements of equilibria in a pure compound

The displacements describing the geometry of a binodal curve are given by

$$\left(\frac{\delta V}{\delta T}\right) = G_{PT} + G_{2P} \left(\frac{\delta P}{\delta T}\right) \quad (S1)$$

$$\begin{aligned} \left(\frac{\delta^2 V}{\delta T^2}\right) = & G_{P2T} + 2G_{2PT} \left(\frac{\delta P}{\delta T}\right) + G_{3P} \left(\frac{\delta P}{\delta T}\right)^2 + \dots \\ & \dots + G_{2P} \left(\frac{\delta^2 P}{\delta T^2}\right) \end{aligned} \quad (S2)$$

$$\left(\frac{\delta P}{\delta T}\right) = -\frac{\Delta A_T}{\Delta V} \quad (S3)$$

and

$$\left(\frac{\delta^2 P}{\delta T^2}\right) = -\frac{\Delta G_{2T} + 2\Delta G_{PT} \left(\frac{\delta P}{\delta T}\right) + \Delta G_{2P} \left(\frac{\delta P}{\delta T}\right)^2}{\Delta V} \quad (S4)$$

where the required Legendre transforms are<sup>1</sup>

$$G_{PT} = -\frac{A_{VT}}{A_{2V}} \quad (S5)$$

$$G_{2P} = -\frac{1}{A_{2V}} \quad (S6)$$

$$G_{P2T} = -\frac{A_{V2T}}{A_{2V}} + 2\frac{A_{2VT}A_{VT}}{A_{2V}^2} - \frac{A_{3V}A_{VT}^2}{A_{2V}^3} \quad (S7)$$

$$G_{3P} = -\frac{A_{3V}}{A_{2V}^3} \quad (S8)$$

$$G_{2PT} = \frac{A_{2VT}}{A_{2V}^2} - \frac{A_{3V}A_{VT}}{A_{2V}^3} \quad (S9)$$

#### S2. Computational cost and comparisons of the proposed methodology with the method of Topliss *et al.*

Let us consider as an example the Carnahan-Starling van der Waals EOS (CS-vdW EOS)<sup>2</sup> with the parameters reported by Topliss *et al.*<sup>3</sup> for methane and apply both the proposed approach and the approach equivalent to the method of Topliss *et al.* The latter is based on the classification of roots and the domain contraction methodology. The procedure can be arranged as follows:

1. Parameters of the model are calculated, and fugacity coefficients is evaluated.
2. The parameter  $\rho_{lim}$  is obtained.
3. The temperature is fixed.
4. For evaluating the isotherm geometry,  $dP/d\rho$  and  $d^2P/d\rho^2$  at  $\rho = 10^{-4}\rho_{lim}$  is obtained. Remarkable, for the considered EOS implemented to pure fluids, only the type-A curves (according to classification of Topliss *et al.*) is obtained until the critical isotherm. Since the pertinent verification is trivial, only the initial values for both phases is determined.
5. An initial value of  $\rho_{lim}/2$  can be used for obtaining  $\rho_{inf}$ . This idea is merely geometric, and it is not described by Topliss *et al.*<sup>3</sup>.
6. The low-density and high-density limits is obtained. The low-density limit is situated between  $\rho_{lb}$  and  $\rho_{inf}$ , while the high-density limit – between  $\rho_{inf}$  and  $\rho_{lim}$ , determining thus the stability areas of a model. Such a procedure is not required by the proposed approach because each approximation rests in a point fulfilling  $A_{2V} > 0$ .
7. Finally, this method is reduced to finding the roots in a manner similar to the proposed one. In order to compare both methods at the same conditions, let us use the conjugate gradient approach for solving the roots, while  $(\rho_{min} + \rho_{lb})/2$

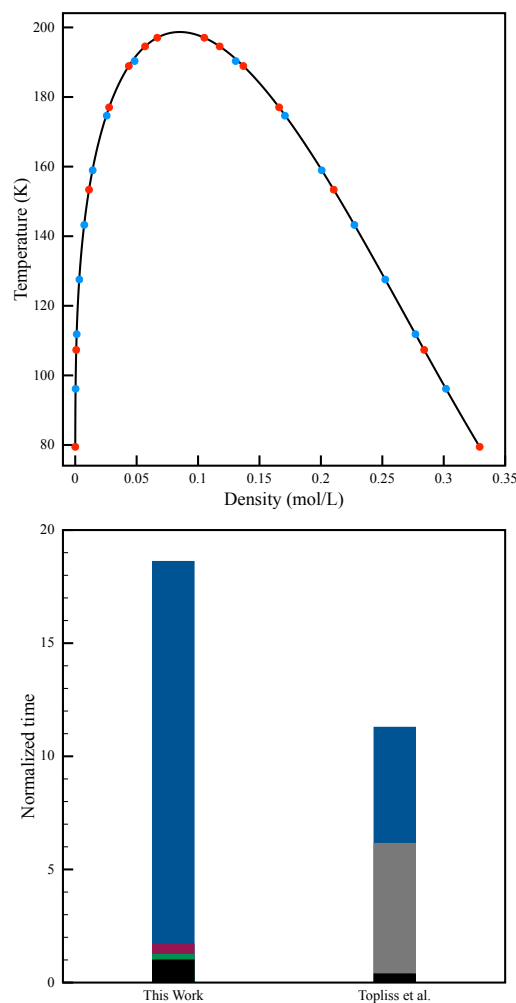
and  $(\rho_{lim} + \rho_{ub})/2$  are used as initial approximations.

Figure S1(a) depicts the results of both approaches, covering the range between  $0.4T_c$  until  $T_c$  and Figure S1(b) compares the CPU times. As seen, in this simple case the proposed method is around 33% slower. However, in the cases of more sophisticated models, such as the IAPWS95 formulation and some SAFT-family EOS that exhibit multiple roots, the domain contraction may fail. Yet the most evident problem of Topliss *et al.* method is the absence of a limit density,  $\rho_{lim}$ . Figure S2 presents a topological analysis of the isotherms exhibited by IAPWS95 formulation. To compare both methods,  $\rho_{lim}$  is considered as the liquid density at the triple point, which requires a previously solved equilibrium point. As seen, multiple  $\rho_{inf}$ ,  $\rho_{ub}$  and  $\rho_{lb}$  appear, which hinders a systematic classification of isotherms. In other words, application of Topliss *et al.* method without previous knowledge of the isotherm geometry is questionable because the procedure easily approaches the non-physical solutions (see the binodal curve represented by black dotted line in Figure S2). Their discontinuity is characterized by  $A_{4V} = \infty$  and it lasts until 639.32 K. Unlike that, the proposed method is free of this problem because it requires only a healthy critical point. Figure S3 depicts its application to the IAPWS95 formulation and the normalized time.

As discussed, application of the Topliss *et al.*<sup>3</sup> approach requires preliminary manual mapping of the EOS behavior to prevent getting of unphysical equilibriums. The relative slowness of the proposed approach is recognized as a reasonable price for a possibility of its fully automatic implementation to even most sophisticated EOS models, including those exhibiting numerical pitfalls and the related phenomena<sup>4</sup>.

Another example of problems associated with a domain contraction is implementation of empirical expressions of vapor pressures providing initial estimations for sophisticated models characterized by non-physical solutions at some specific temperatures. Let us consider again the IAPWS formulation for water with a triple point packing fraction and the DIPPR Equation 101<sup>5</sup>. However, this time an equilibrium is calculated at 580 K only. Having this temperature and the pertinent initial estimation of DIPPR Equation 101 for the pressure (94.585 bar). However, considering fixed temperature and pressure, it is not always possible to find an inflection point of the isotherm. For this reason, a root of the isotherm at the fixed pressure is considered as  $\rho_{inf}$ . Besides that, multiple solutions are found (see Table S1).

*Solution 1* represents a non-physical equilibrium point obtained using a simple domain contraction approach. Although *Solution 2* is a non-physical equilibrium point as well, it is obtained while considering an additional criterion, namely  $A_{2V} > 0$ , in order to guarantee



**Figure S1:** (a) Binodal curve of methane as predicted by CS-vdW EOS, black line: our approach using  $\kappa_2 = 0.05$ , **crimson symbols:** our method using  $\kappa_2 = 1.00$  and **blue symbols:** seven equilibrium points calculated by Topliss *et al.* approach. (b) Normalized time for Topliss *et al.* and our approach using the CS-vdW EOS for methane. Colors are **black**, evaluation of the model, parameters and fugacity coefficients; **green**, calculation of the critical point; **red**, calculation of the first initial values; **grey**, classification of the roots and stability areas of the isotherm and **blue**, calculation of the diagram.

**Table S1:** The solutions found by a domain contraction approach and DIPPR Equation 101<sup>5</sup> for providing an initial value for solving IAPWS formulation at 580 K.

	$\rho^l$	$\rho^v$
	mol/L	
<i>Solution 1</i>	31.5108	2.99788
<i>Solution 2</i>	38.4434	7.03842
<i>Solution 3</i>	38.7248	2.87196

that the segment of an isotherm is locally stable. To achieve the physical *Solution 3*, four domain contractions are performed and, additionally, it includes the  $A_{2V} > 0$  criterion. The latter requires preliminary information of the isotherm behavior. The three equilibrium points shown in Table S1 are graphically rep-

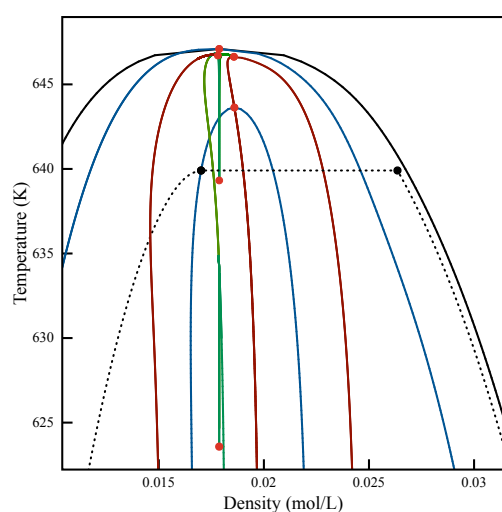
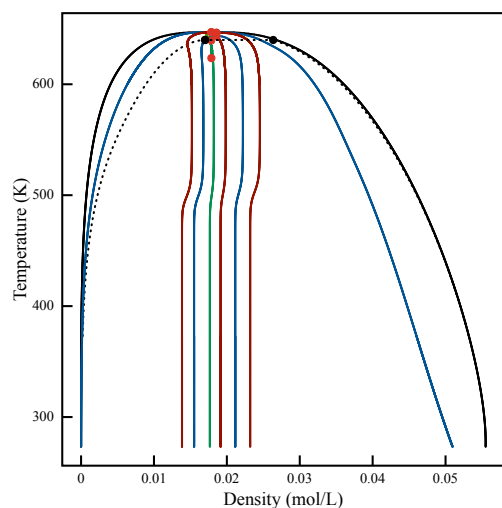


**Figure S2:** Topological analysis of the isotherms of the IAPWS approach. **Black continuous line:** actual phase diagram predicted by the model, **black discontinuous line:** additional non-physical equilibrium predicted by the model, **blue lines:** extremal values of the isotherms, **crimson lines:** changes of the concavities of the isotherms, **green lines:** singular points on the isotherms. (a): from triple point till critical point and (b) the neighborhood of the critical point.

resented in Figure S4.

### S3. Wolfram Mathematica<sup>®</sup> code

The derivatives of the Helmholtz energy function can be obtained using the symbolic derivative command of Wolfram Mathematica<sup>®</sup>.

```
Av=D[A,v];
A2v=D[Av,v];
A3v=D[A2v,v];
A4v=D[A3,v];
A5v=D[A4,v];
AT=D[A,T];
A2T=D[AT,T];
AvT=D[Av,T];
A2vT=D[AvT,v];
A3vT=D[A2vT,v];
```

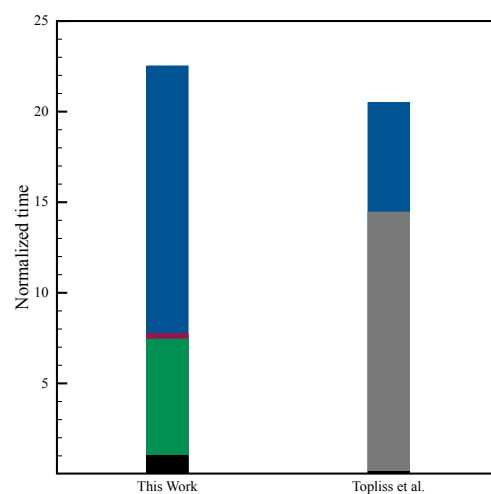
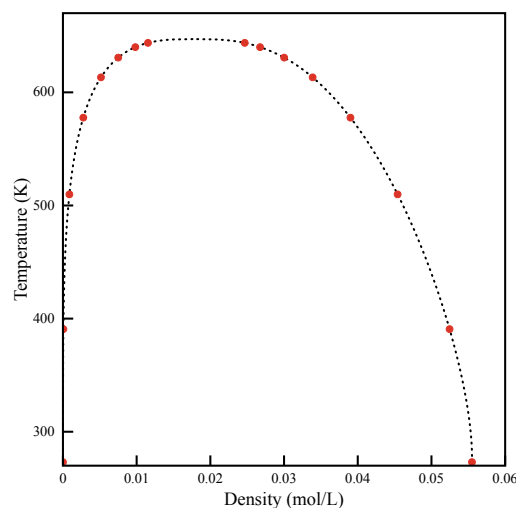


**Figure S3:** (a) Binodal curve of water as predicted by IAPWS EOS, dotted line: the proposed approach using  $\kappa_2 = 0.05$ , crimson symbols: our method using  $\kappa_2 = 1.00$ . (b) Normalized time for Topliss *et al.* and our approach using the IAPWS EOS. Colors concern to: **black**, evaluation of the model, parameters and fugacity coefficients. **green**, calculation of the critical point. **Red**, calculation of the first initial values. **Grey** classification of the roots and stability areas of the isotherm. **Blue**, calculation of the diagram.

```
A4vT=D[A3vT,v];
Av2T=D[AvT,T];
A3v2T=D[A3vT,T];
```

Now, the Gibbs energy function and its derivatives are obtained from Legendre transformations of the Helmholtz energy function as

```
G=A-v Av;
G2P=-1/A2v;
G3P=-A3v/A2v^3;
GPT=-AvT/A2v;
G2TP=-Av2T/A2v+2A2vT AvT/A2v^2-...
...-A3v AvT^2/A2v^3;
GT2P=A2vT/A2v^2-A3v AvT/A2v^3;
G2T=A2T-AvT^2/A2v;
```

For the first stage of the procedure, the estimates of the initial values for the liquid and vapor volumes are given by

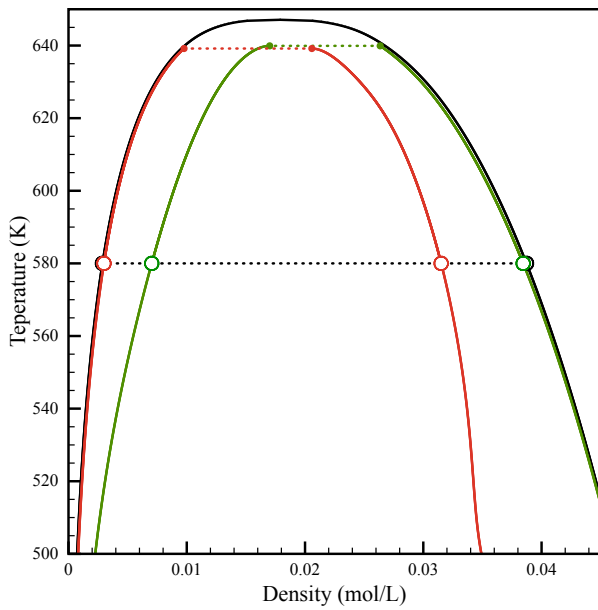


**Figure S4:** The solutions found by a domain contraction approach and the DIPPR Equation 101<sup>5</sup> for providing an initial value for solving IAPWS formulation. In crimson *Solution 1*, in green *Solution 2* and in black the actual *Solution (3)*.

```
v0=Na sigma^3/chi[m];
T0=varepsilon/tau/(1-2/n/m/varepsilon varepsilonAB
betaAB);
Vc=Chop[FindRoot[{A2v,A3v},{v,v0},{T,T0}]];
v0= v/.Vc;
T0=T/.Vc;
Ta=T0-k1(dvdT/d2vdT2)/.{v→v0,T→T0};
va=v0-(1/2)(2-k1)k1(dvdT^2/d2vdT2)/.{v→v0,T→T0};
v10=va-(3A3v)/(2A4v)-Sqrt[9A3v^2-2A4v A4v]/...
.../(2A4v)/.{v→va,T→Ta};
vv0=va-(3A3v)/(2A4v)+Sqrt[9A3v^2-2A4v A4v]/...
... (2A4v)/.{v→va,T→Ta};
```

In addition, the slope and curvature of the vapor pressure are given by

```
dPdT=-1/(vv-v1)((AT/.{v→vv})-(AT/.{v→v1}));
d2PdT2=-1/(vv-v1)((G2T /.{v→vv})-...
...-(G2T/.{v→v1}))+2((GPT/.{v→vv})-...
...-(GPT/.{v→v1}))dPdT+((G2P/.{v→vv})-...
...-(G2P/.{v→v1}))dPdT^2);
```

Finally, the geometric structures of the binodal curve can be expressed as

```
vT=(GPT+G2P dPdT);
v2T=(G2TP+GT2P dPdT+(GT2P+G3P dPdT)dPdT+...
...+G2P d2PdT2);
vTL=vT/.{v→v1};
v2TL= v2T/.{v→v1};
vTV=vT/.{v→vv};
v2TV=v2T/.{v→vv};
ΔTL=-k2 vTL/v2TL;
ΔTV=-k2 vTV/v2TV;
```

and the objective function refining the equilibrium calculations are:

```
of1=(G/.{v→v1})-(G/.{v→vv});
of2=(Av/.{v→v1})-(Av/.{v→vv});
```

In this work,  $k_1$  and  $k_2$  are selected as 1/10 and 1, respectively.

#### S4. Preliminary implementation in mixtures

The implementation of the proposed approach to multicomponent mixtures is straightforward if the geometry of the EOS is previously known. Let us consider an example of the applying the second-order differential accelerators for equilibrium in methane(1) – propane(2) system at 300 K. The parameters used in this example are listed in Table S2.

**Table S2:** Parameters for methane and propane for CS-vdW EOS.

	$a_2^{(0)}$	$a_2^{(1)}$	$a_2^{(2)}$	$b_2^{(0)}$
CH <sub>4</sub> <sup>1</sup>	0.49539	0.16199	0.33333	0.17841
C <sub>3</sub> H <sub>8</sub> <sup>2</sup>	0.53557	0.08105	0.33333	0.16785

1: taken from Topliss *et al.*

2: parametrized for this work.

As in the cases of pure compounds, an accelerator for binary mixtures requires rendering the coexistence curves as differential equations with further approximating equilibrium through the second-order Taylor series. The displacements based on the Malesinski's mathematics are:

$$\left(\frac{\delta x_1^\pi}{\delta P}\right)_T = -\frac{\Delta G_P + G_{xP}^\pi (x_1^\pi - x_1^\alpha)}{(x_1^\pi - x_1^\alpha) G_{2x}^\pi} \quad (S10)$$

$$\left(\frac{\delta^2 x_1^\pi}{\delta P^2}\right)_T = -\frac{1}{(x_1^\pi - x_1^\alpha) G_{2x}^\pi} \left( \phi_1 + \phi_2 \left(\frac{\delta x_1^\pi}{\delta P}\right)_T \right) \quad (S11)$$

where

$$\phi_1 = \frac{\delta \Delta G_P}{\delta P} + \frac{\delta G_{xP}^\pi}{\delta P} (x_1^\pi - x_1^\alpha) + G_{xP}^\pi \left( \frac{\delta x_1^\pi}{\delta P} - \frac{\delta x_1^\alpha}{\delta P} \right) \quad (S12)$$

$$\phi_2 = \frac{\delta G_{2x}^\pi}{\delta P} (x_1^\pi - x_1^\alpha) + G_{2x}^\pi \left( \frac{\delta x_1^\pi}{\delta P} - \frac{\delta x_1^\alpha}{\delta P} \right) \quad (S13)$$

where  $\pi$  refers to any (vapor or liquid) phase, while  $\alpha$  is a phase exhibiting equilibrium with the  $\pi$ -phase. Obviously, the method can be applied for LLE as well. In addition, the volume displacements are:

$$\left(\frac{\delta v^\pi}{\delta x_1}\right)_T = G_{xP}^\pi + G_{2P}^\pi \left(\frac{\delta P}{\delta x_1^\pi}\right)_T \quad (S14)$$

$$\left(\frac{\delta^2 v^\pi}{\delta (x_1^\pi)^2}\right)_T = \frac{\delta G_{xP}^\pi}{\delta x_1} + \frac{\delta G_{2P}^\pi}{\delta x_1} \left(\frac{\delta P}{\delta x_1^\pi}\right)_T + \dots \quad (S15)$$

$$\dots + G_{2P}^\pi \left(\frac{\delta^2 P}{\delta (x_1^\pi)^2}\right)_T$$

The curvature around the critical point required for initializing the proposed method can be obtained as:

$$\left(\frac{\partial P}{\partial x_1}\right)_c = \kappa_1 \frac{\Delta x_1}{6} \left(\frac{\partial^4 G}{\partial x_1^4}\right) \left(\frac{\partial^3 G}{\partial x_1^3 \partial P}\right) \quad (S16)$$

where  $\Delta x_1$  is some small number (in this example taken as 0.01) and  $\kappa_1 = 1/100$ . As discussed, the proposed method becomes advantageous in the cases of much more sophisticated models. Its implementation to such models for calculating phase equilibria in multi-compound systems will be presented in a forthcoming study.

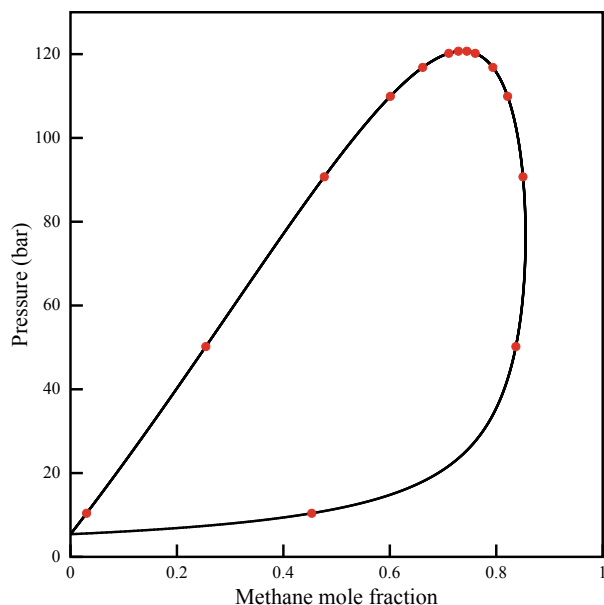


**Figure S5:** Phase diagram of the methane(1) – propane(2) system at 300 K as predicted by CS-vdW EOS.

## Nomenclature

$\rho_{lim}$ : EOS specific parameter characterized by  $P(\rho) = \infty$ .

$\rho_{inf}$ : point of the isotherm given by  $d^2P/d\rho^2 = 0$ .

$\rho_{ub}$ : high-density limit for determinate an initial value of the liquid phase.

$\rho_{lb}$ : low-density limit for determinate an initial value of the liquid phase.

## References

- (1) Reid, R. C.; Beegle, B. L. Critical point criteria in Legendre transform notation. *AIChE J.* **1977**, *23*, 726–732.
- (2) Dimitrelis, D.; Prausnitz, J. M. Comparison of two hard-sphere reference systems for perturbation theories for mixtures. *Fluid Phase Equilib.* **1986**, *31*, 1–21.
- (3) Topliss, R. J.; Dimitrelis, D.; Prausnitz, J. M. Computational aspects of a non-cubic equation of state for phase-equilibrium calculations. Effect of density-dependent mixing rules. *Comput. Chem. Eng.* **1988**, *12*, 483–489.
- (4) Imre, A. R.; Groniewsky, A.; Györke, G. Description of the metastable liquid region with quintic and quasi-quintic equation of states. *IPHT* **2017**, *5*, 173–185.
- (5) DIPPR: The Design Institute for Physical Properties, DIPPE 801 thermophysical property database and DIADEM predictive software. 2007.